Magnetism, electronic transport, and colossal magnetoresistance of $(La_{0.7-x}Gd_x)Sr_{0.3}MnO_3$ ($0 \leq x \leq 0.6$)

Young Sun and M. B. Salamon

Department of Physics and Materials Research Laboratory, University of Illinois at Urbana-Champaign, 1110 West Green Street, Urbana, Illinois 61801-3080

Wei Tong and Yuheng Zhang

Structure Research Laboratory, University of Science and Technology of China, Hefei, Anhui 230026, People's Republic of China

The magnetic and electronic properties of the perovskite system $(La_{0.7-x}Gd_x)Sr_{0.3}MnO_3$ ($0 \leq x \leq 0.6$) have been investigated by measurements of magnetization, resistivity and magnetoresistance. The substitution of Gd on La sites not only results in a decrease of the Curie temperature T_c and the magnetization, but also induces cluster-glass and ferrimagnetic behaviors. For $x \leq 0.15$, the system is metallic below 300 K, while for $0.2 \leq x \leq 0.4$, there is an insulating-metallic transition. For $x \geq 0.5$, the system is insulating. For $x \geq 0.3$, the resistivity in the paramagnetic regime can be fitted by variable-range hopping model. Both the high-field (6 T) and low-field (1 T) magnetoresistances are significantly enhanced by Gd substitution. The steep insulating-metallic transition in $x=0.3$ and 0.4 samples gives rise to a large temperature coefficient of resistance. Infrared spectra measurements provide strong evidence of the change of Mn-O-Mn bond angle due to Gd substitution. These results suggest that both the average A-site ionic radius (tolerance factor) and the additional magnetic coupling between Gd^{3+} and Mn^{3+}/Mn^{4+} sublattice are important factors in determining the magnetic and electronic states. The enhancement of colossal magnetoresistance and *I-M* transition are interpreted based on the scenario of phase separation.

I. INTRODUCTION

The mixed valent manganites with the general formula $La_{1-y}A_yMnO_3$ and perovskite structure have drawn much research interest due to their unusual electronic and magnetic properties, colossal magnetoresistance (CMR),[1–3] charge ordering,[4,5] orbital ordering,[6,7] and phase separation[8–10] in particular. The parent compound $LaMnO_3$ is well known to be an antiferromagnetic insulator. When a fraction of the trivalent lanthanum ions are replaced by divalent ions such as Ca, Sr, or Ba, $La_{1-y}A_yMnO_3$ exhibits a rich and complex phase diagram. Within a broad doping level $0.2<y<0.5$, an insulating-metallic (*I-M*) transition associated with a paramagnetic-ferromagnetic (PM-FM) transition occurs and the colossal magnetoresistance effect appears just around it. The origin of ferromagnetism and the close correlation between the magnetic and transport properties in $La_{1-y}A_yMnO_3$ are basically interpreted within the framework of double exchange model,[11] which considers the transfer of an e_g electron between neighboring Mn^{3+} and Mn^{4+} ions. In addition, the strong electron-phonon interaction due to the Jahn-Teller effect is also believed to play a key role in these manganites.[12]

The electronic and magnetic states of $La_{1-y}A_yMnO_3$ depend on both the hole density (i.e., the A^{2+} doping level) and the tolerance factor. The tolerance factor, defined as $t = \langle A\text{-}O \rangle / \sqrt{2} \langle Mn\text{-}O \rangle$, where $\langle A\text{-}O \rangle$ and $\langle Mn\text{-}O \rangle$ are the mean cation-oxygen bond lengths of A site (La^{3+} and A^{2+}) and Mn site respectively, reflects the local microscopic distortions from ideal cubic perovskite structure ($t=1$). The optimum A^{2+} doping level is close to 0.3, where the double-

exchange FM interaction reaches its maximum. With decreasing t, the Mn-O-Mn bond angle decreases, which affects the transfer integral between Mn^{3+} and Mn^{4+} ions. While maintaining the optimum A^{2+} doping level, one can tune the tolerance factor by replacing La with smaller rare-earth ions. There have been systematic studies of the $(La_{1-x}R_x)_{0.7}Ca_{0.3}MnO_3$ system. Hwang *et al.*[13] investigated the tolerance factor dependence of the electronic and magnetic states in $(La_{1-x}R_x)_{0.7}Ca_{0.3}MnO_3$ by replacing La^{3+} with some light rare-earth ions Pr^{3+} and Y^{3+}. They found that the FM Curie temperature T_C and conductivity decrease with increasing Pr^{3+} or Y^{3+} content and established a T_C-t phase diagram. Terai *et al.* studied the $(La_{1-x}Dy_x)_{0.7}Ca_{0.3}MnO_3$ system and found some effects different from compounds containing light rare-earth ions.[14] Terashita *et al.* recently investigated the $(La_{1-x}Gd_x)_{0.7}Ca_{0.3}MnO_3$ system and suggested that phase segregation leads to a disagreement between metal-insulator transition and ferromagnetic transition temperature.[15]

Similar studies in another prototype CMR system $(La_{0.7-x}R_x)Sr_{0.3}MnO_3$ are still not complete,[16] especially those containing heavy rare-earth ions. Due to the much smaller ionic radius and high magnetic moment, the replacement of La by a heavy rare-earth element will not only influence the lattice distortion but also introduce extra magnetic coupling. In this paper, we present a detailed study of Gd-substituted system $(La_{0.7-x}Gd_x)Sr_{0.3}MnO_3$ ($0.0 \leq x \leq 0.6$), with the measurents of magnetization, resistivity, magnetoresistance, and infrared spectra. The purpose is to study the dependence of magnetic and electronic transport behaviors on the tolerance factor (controlled by the average
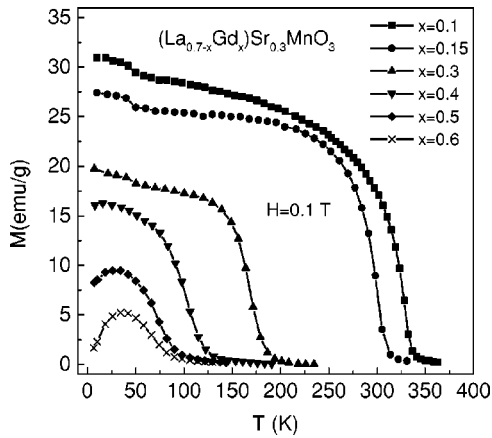
FIG. 1. Temperature dependence of magnetization in 0.1 T field for $(La_{0.7-x}Gd_x)Sr_{0.3}MnO_3$.

FIG. 2. Temperature dependence of magnetization in 0.01 T field for $(La_{0.5}Gd_{0.2})Sr_{0.3}MnO_3$ in both ZFC and FC processes.

A-site ionic radius) as well as the effects of the extra rare-earth magnetic moment that has usually been ignored.

II. EXPERIMENT

Polycrystalline samples of $(La_{0.7-x}Gd_x)Sr_{0.3}MnO_3$ ($x = 0.0, 0.05, 0.1, 0.15, 0.2, 0.3, 0.4, 0.5,$ and 0.6) were prepared by the standard solid state reaction method. Stoichiometric mixtures of high purity La_2O_3, Gd_2O_3, $SrCO_3$, and MnO_2 were first heated at $800°C$ for 12 h, then at $1000°C$ for 12 h and at $1200°C$ for another 12 h, with intermediate grinding. Finally, after being ground and pressed into pellets, the samples were sintered at $1380°C$ for 36 h. The structure and phase purity of as-prepared samples were checked by powder x-ray diffraction (XRD) at room temperature. The XRD patterns indicate single phase rhombohedral structure for low-doped ($x < 0.2$) samples and orthorhombic structure for high-doped ($x \geq 0.2$) samples. The magnetization was measured using a Lakeshore vibrating sample magnetometer. Resistivity was measured by standard four-probe method. Infrared spectra were taken in the frequency range from 350 to 1000 cm^{-1} at room temperature.

III. RESULTS

A. Magnetism

We first investigated the magnetic properties. In Fig. 1, we show the temperature dependence of magnetization in 0.1 T magnetic field for $(La_{0.7-x}Gd_x)Sr_{0.3}MnO_3$ ($x = 0.1, 0.15, 0.3, 0.4, 0.5,$ and 0.6). With increasing Gd content, the PM-FM transition shifts to lower temperature and the magnetization decreases. The Curie temperatures T_c,
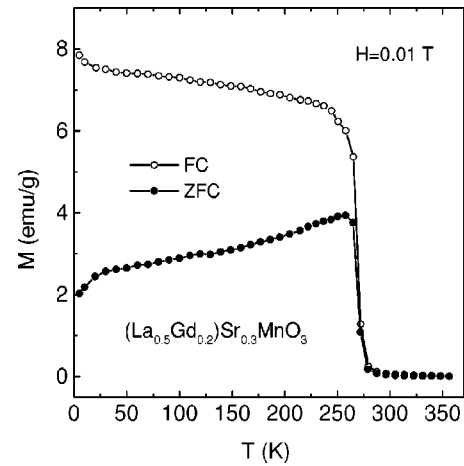
which are defined as the inflection point in M-T curves, are summarized in Table I. In order to identify the exact magnetic structure after the ferromagnetic ordering, we intentionally measured the magnetization of the $x = 0.2$ sample with low field (0.01 T) in both zero-field cooled (ZFC) and field cooled (FC) process, as shown in Fig. 2. It is clear that the FC curve does not coincide with ZFC curve just below T_c. The large discrepancy between ZFC and FC magnetization is usually understood as a sign of spin–cluster-glass state that has no simple long-range ferromagnetic ordering.[17] The decrease of the Curie temperature and magnetization with the replacement of La by smaller rare-earth ions has been observed in previous studies.[13–16] The usual interpretation is that the smaller average A-site ionic radius causes a larger distortion of the Mn-O-Mn bond and consequently weakens the double exchange interaction. Apart from the above mechanism, we believe that the large local moment of Gd^{3+} ions should play a key role in the magnetic behavior. To clarify it, we also measured the M-H curves for both low-doped ($x = 0.2$) and high-doped ($x = 0.5$) samples. As shown in Fig. 3, for the $x = 0.2$ sample, M rises up dramatically at low field and tends to saturate at high field. However, for the $x = 0.5$ sample, the $M-H$ behavior is quite different: after a steep rise in the low field range ($H \leq 0.1$ T), the magnetization still increases steadily with increasing magnetic field and does not show any sign of saturation, even at low temperature ($T = 10$ K). The continuous increase of M with high magnetic field and the small value of it indicate a ferrimagneticlike state in high-doped samples. Assuming a pure ferrimagnetic state (the moments of Gd^{3+} and Mn^{3+}/Mn^{4+} are absolutely opposite), we expect the net magnetization of

TABLE I. Curie temperature T_c, I-M transition temperature T_p, and the fitting parameter T_0 to Mott's law, of $(La_{0.7-x}Gd_x)Sr_{0.3}MnO_3$.

Sample	$x = 0.1$	$x = 0.15$	$x = 0.2$	$x = 0.3$	$x = 0.4$	$x = 0.5$	$x = 0.6$
T_c	328	298	270	168	104	74	66
T_p			270	185	120		
T_0				4.3×10^7	8.8×10^7	1.1×10^8	1.3×10^8
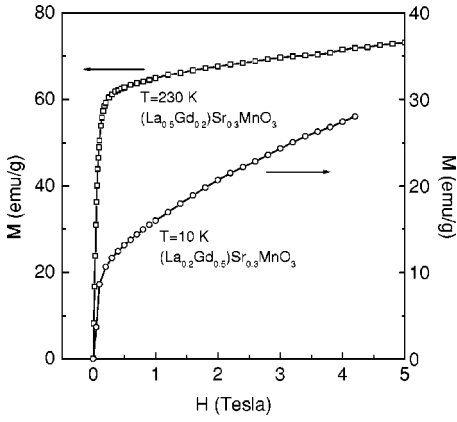
FIG. 3. *M-H* curves of $(La_{0.5}Gd_{0.2})Sr_{0.3}MnO_3$ and $(La_{0.2}Gd_{0.5})Sr_{0.3}MnO_3$.

$(La_{0.2}Gd_{0.5})Sr_{0.3}MnO_3$ to be 4.7 emu/g. This value is considerably lower than the experimental data ~ 8.5 emu/g at the low field regime (~ 0.1 T). This discrepancy may suggest that the Gd content is slightly smaller than 0.5. If in a pure ferrimagnetic state, the magnetization of 8.5 emu/g corresponds to a Gd content of $x=0.48$. Another possibility is that a spin-canted structure, rather than a pure ferrimagnetic state, exists in the present sample. We note that previous studies of Gd-doped La-Ca-Mn-O have shown a spin-canted structure in low-doped samples[18] and a ferrimagnetic state in $Gd_{0.67}Ca_{0.33}MnO_3$.[19] The spin-canted or the ferrimagnetic state suggest that the exchange coupling between the Gd^{3+} and the Mn^{3+}/Mn^{4+} sublattices tends to be antiferromagnetic.

B. Electronic transport

In Fig. 4, we demonstrate the temperature dependence of resistivity without magnetic field for all samples. The resistivity increases with increasing Gd content. When $x \leqslant 0.15$, the samples show metallic behavior below 300 K. For $0.2 \leqslant x \leqslant 0.4$, an insulator-metal transition was observed. When
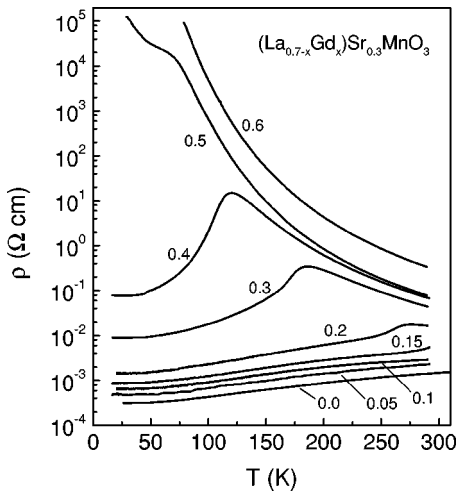

FIG. 4. Temperature dependence of the resistivity in zero field for all samples.
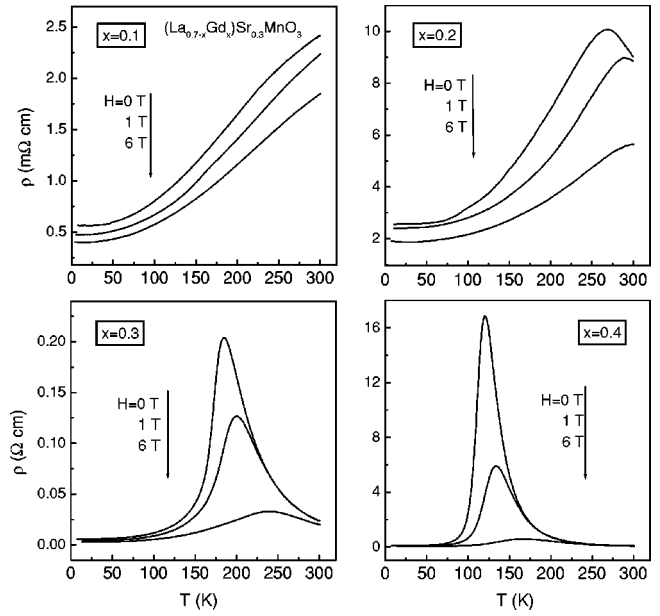

FIG. 5. Temperature dependence of the resistvity under magnetic fields for several typical samples.

$x \geqslant 0.5$, the samples are insulating, though an apparent slope change of resistivity was observed for $x=0.5$. To study the magnetoresistance effect, we also measured the resistivity of several typical samples under different magnetic fields, as shown in Fig. 5. For $(La_{0.6}Gd_{0.1})Sr_{0.3}MnO_3$, which has a T_c above room temperature, the behavior is metallic below 300 K and the magnetoresistance is relatively small. For $(La_{0.5}Gd_{0.2})Sr_{0.3}MnO_3$, there is an *I-M* transition just at T_c (270 K) and the CMR appears mainly around T_c. With further Gd content, $(La_{0.4}Gd_{0.3})Sr_{0.3}MnO_3$ and $(La_{0.3}Gd_{0.4})Sr_{0.3}MnO_3$ exhibit enhanced *I-M* transition so that the resistivity shows a sharp peak at a temperature T_p. For $(La_{0.4}Gd_{0.3})Sr_{0.3}MnO_3$ and $(La_{0.3}Gd_{0.4})Sr_{0.3}MnO_3$, T_p is 185 and 120 K, respectively, much above their Curie temperatures (168 and 104 K). We note that the discrepancy between T_c and the *I-M* transition temperature T_p has also been observed in $(La_{1-x}Gd_x)_{0.7}Ca_{0.3}MnO_3$ when $x \geqslant 0.2$ and was interpreted as a result of phase segregation.[15] It is also worthwhile to compare Curie temperature T_c with the temperature at which $d\rho/dT$ reaches a maximum. For $(La_{0.4}Gd_{0.3})Sr_{0.3}MnO_3$ and $(La_{0.3}Gd_{0.4})Sr_{0.3}MnO_3$, this temperature is 172 and 111 K, respectively, very close to their T_c's, which implies that the *I-M* transition is triggered by magnetic ordering.

For $x \geqslant 0.3$, the resistivity shows insulating behavior over a substantial temperature interval so that we can fit it with different models. We first tried with the adiabatic small polaron hopping model[20] $\rho = BT \exp(E_a/kT)$. As shown in Fig. 6(a), the nonlinear shape of these plots suggests that the resistivity in the paramagnetic regime does not obey the small polaron model well. In contrast, the Mott's variable-range hopping model,[21] $\rho = \rho_0 \exp(T_0/T)^{1/4}$, can give a better fitting to the resistivity. As seen in Fig. 6(b), except for $x=0.5$, the resistivity in the paramagnetic regime can be fitted by Mott's law very well. This result indicates that Gd dopping causes
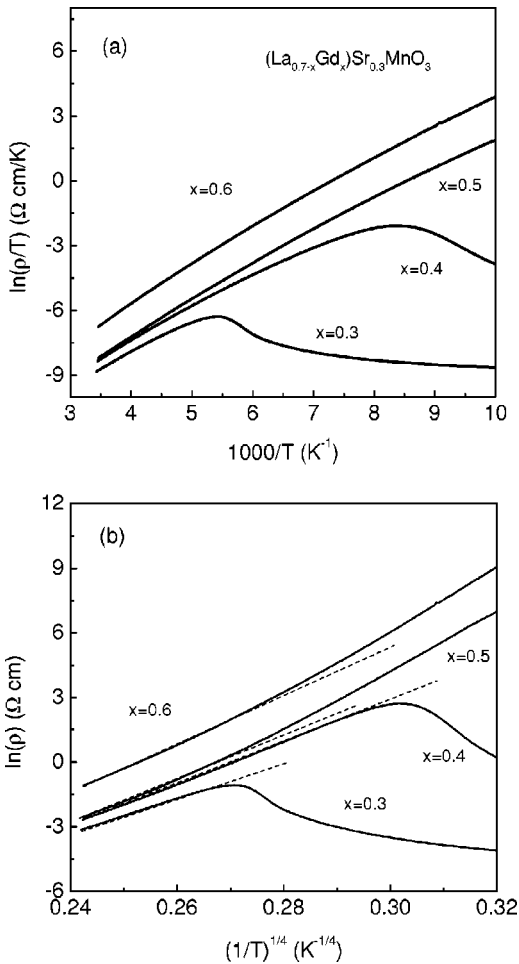
FIG. 6. (a) $\ln(\rho/T)$ versus $1/T$ and (b) $\ln(\rho)$ versus $1/T^{-1/4}$, for $x \geq 0.3$ samples. The dashed lines are fits to Mott's law.

strong potential fluctuation which is favorable to the variable-range hopping. The fitting parameter T_0, as summarized in Table I, is related to localization length L by the expression $kT_0 = 18/[L^3 N(E)]$, where k is Boltzman constant, $N(E)$ is the electronic density of states. Since Gd doping does not change the Mn^{3+}/Mn^{4+} ratio, it is reasonable to assume that $N(E)$ is nearly independent on Gd content. Therefore, the variation of T_0 with Gd content reflects the change of localization length. From Table I, one can see that T_0 increases with increasing Gd content. This implies that the disorder in the lattice grows up with Gd doping.

The enhanced I-M transition in $(La_{0.7-x}Gd_x)Sr_{0.3}MnO_3$ is very sensitive to applied magnetic field. From Fig. 5 one can see that the resistivity peak is significantly depressed by applied magnetic field, which leads to an enormous enhancement of the CMR effect. The corresponding MR ratio is plotted in Fig. 6. As shown in Figs. 7(a) and 7(b), the maximum MR ratio in 6 T field is $\sim 8300\%$ at 117 K for $(La_{0.3}Gd_{0.4})Sr_{0.3}MnO_3$ and $\sim 930\%$ at 182 K for $(La_{0.4}Gd_{0.3})Sr_{0.3}MnO_3$. Even in 1 T field, the MR ratio is as high as 520 and 150% for $(La_{0.3}Gd_{0.4})Sr_{0.3}MnO_3$ and $(La_{0.4}Gd_{0.3})Sr_{0.3}MnO_3$, respectively.

In addition to the CMR, the sharp drop of resistivity at the insulator-metal transition results in a large temperature coef-
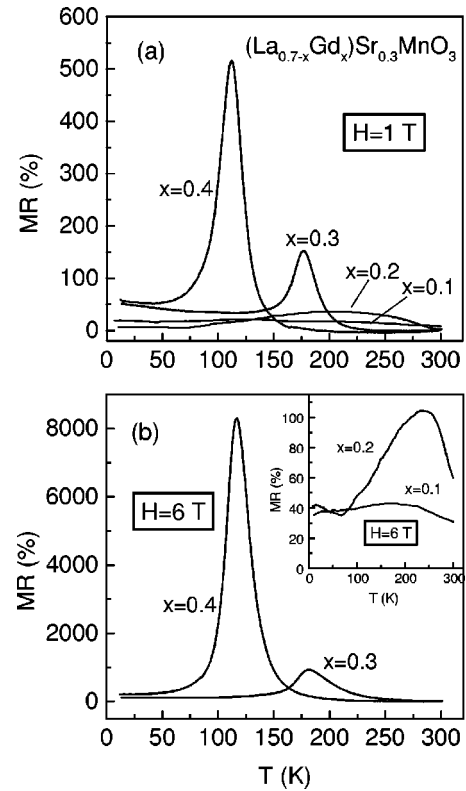

FIG. 7. Temperature dependence of the MR ratio in (a) 1 T magnetic field and (b) 6 T magnetic field, for $(La_{0.7-x}Gd_x)Sr_{0.3}MnO_3$ ($x = 0.1$, 0.2, 0.3, and 0.4).

ficient of resistance [TCR, defined as $(dR/dT)/R$], which is beneficial for bolometric applications.[22–24] As shown in Fig. 8, the maximum of TCR is $\sim 15\%$ and $\sim 7.5\%/K$ for $(La_{0.3}Gd_{0.4})Sr_{0.3}MnO_3$ and $(La_{0.4}Gd_{0.3})Sr_{0.3}MnO_3$, respectively. Since bolometric applications require thin films and the TCR is usually larger in thin film samples,[22] one may expect a higher TCR in $(La_{0.7-x}Gd_x)Sr_{0.3}MnO_3$ thin films.
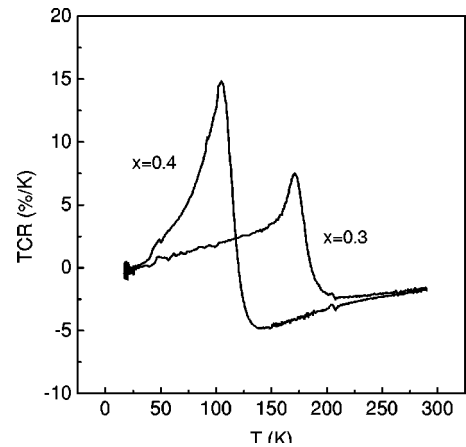

FIG. 8. Temperature dependence of the TCR, defined as $(dR/dT)/R$, for $(La_{0.7-x}Gd_x)Sr_{0.3}MnO_3$ ($x = 0.3$ and 0.4) bulk samples.
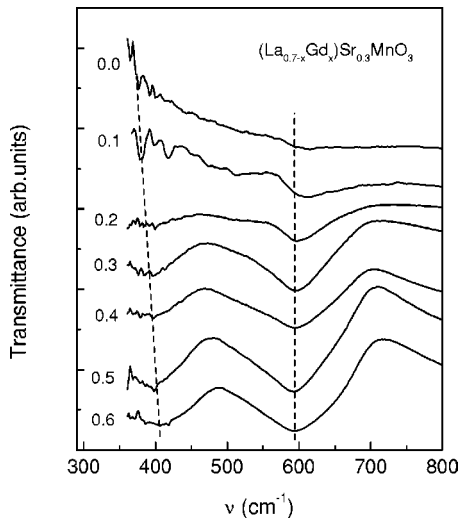
FIG. 9. Infrared spectra of $(La_{0.7-x}Gd_x)Sr_{0.3}MnO_3$ at room temperature.

IV. DISCUSSION

As generally recognized in previous studies, the smaller ionic radius of Gd^{3+} compared to La^{3+} leads to the decrease of the tolerance factor with increasing Gd content, which results in bending of the Mn-O-Mn bond angle. In order to see how the bond angle varies with Gd substitution, we measured the infrared absorption spectra at room temperature for $(La_{0.7-x}Gd_x)Sr_{0.3}MnO_3$, shown in Fig. 9. The bending mode ν_4, located around 390 cm^{-1}, reflecting an internal motion of Mn and O ions located along a particular direction against the other oxygen ions in a plane perpendicular to that direction, is highly sensitive to a change in the Mn-O-Mn bond angle. The streching mode ν_3 located near 600 cm^{-1}, corresponding to an internal motion of Mn ion against the oxygen octahedron, is sensitive to the Mn-O bond length.[25] The signal from $x=0.0$ and 0.1 samples is weak because their T_c's are above room temperature. With increasing Gd content, the bending mode broadens and shifts while the streching mode hardly moves. This result suggests that the substitution of Gd on La sites mainly influences the Mn-O-Mn bond angle rather than the Mn-O bond length. The shift of the bending mode has its direct consequence in the transport properties. When the shift of bending mode is slight ($x\leqslant0.1$), the resistivity is metallic. For $0.2\leqslant x\leqslant0.4$, the further shift of bending mode results in an *I-M* transition. The transition temperature decreases with increasing shift of the bending mode. For $x\geqslant0.5$, the bending mode shifts more and no *I-M* transition occurs. The infrared spectra demonstrates that the Mn-O-Mn bond angle is a critical factor in determining the electronic and magnetic state.

The significant enhancement of the magnetoresistance, especially the low-field magnetoresistance, in $(La_{0.7-x}Gd_x)Sr_{0.3}MnO_3$ samples, is important for practical applications and also informative as to the mechanism of CMR in perovskite manganites. Recent intensive studies have shown that a phase separation underlies the *I-M* transition and CMR in perovskite manganites,[8,9,26,27] i.e., spatially inhomogeneous metallic and insulating areas coexist

and the percolation of metallic ferromagnetic clusters with temperature or by applied field leads to the *I-M* transition and CMR. Even when La is replaced by other rare-earth elements, phase separation and percolative conduction still appear.[15,28,29] This phase separation has been proposed to originate from the disorder due to the different ionic radius of various elements that compose the manganites.[8,27] Moreover, Salamon[30] recently emphasized the thermodynamic feature of the percolating entities and proposed that the magnetic transition and CMR effect should be viewed in the context of the Griffiths singularity driven by intrinsic randomness.

As described in Sec. III, there is a disagreement between *I-M* transition and ferromagnetic transition temperature in $(La_{0.7-x}Gd_x)Sr_{0.3}$ MnO_3 ($x\geqslant0.2$). The same effect was found in $(La_{1-x}Gd_x)_{0.7}Ca_{0.3}MnO_3$ ($x\geqslant0.2$), where it was believed to result from phase segregation.[15] Based on the scenario of phase separation, the role of Gd in the enhancement of the *I-M* transition and CMR may be comprehended from two sides. On the one hand, the decrease of average A-site ionic radius (i.e., the decrease of the tolerance factor t) with increasing Gd content leads to the gradual bending of the Mn-O-Mn bond, which causes the enhancement of the effective Jahn-Teller electron-phonon coupling and results in a reduced mobility of the carriers.[31] Meanwhile, the doping of Gd promotes the random character of the distribution of A-site ions (La^{3+},Sr^{2+},Gd^{3+}), leading to the random distribution of hoppings and exchange between the localized spins. As discussed in Ref. 27, the cluster size in the phase separation regime is governed by the strength of disorder (the smaller the disorder, the larger the cluster size). Therefore, the increase of disorder induced by Gd substitution will definitely influence the cluster size in the phase separation regime. On another hand, the substitution of nonmagnetic La^{3+} by magnetic Gd^{3+} would introduce extra magnetic coupling since Gd^{3+} has a large local moment. The cluster glasslike behavior and the ferrimagnetic feature introduced by Gd substitution suggest an antiferromagnetic exchange coupling between Gd^{3+} and Mn^{3+}/Mn^{4+} sublattice. The competing antiferromagnetic coupling would also contribute to the disorder in the lattice and influence the cluster size in the phase separation regime.

Therefore, as the extent of disorder grows with Gd doping, we may expect that the cluster size reduces. This means that the phase separation around T_c in $(La_{0.7-x}Gd_x)Sr_{0.3}MnO_3$ is in the form of many small isolated metallic clusters, coexisting with insulating areas. Due to the lower T_c caused by Gd doping and the fact that the percolation point is consistent with T_c, the small metallic clusters would accumulate while the resistance of the insulating phase keeps increasing before reaching T_c. When a large number of small metallic clusters percolate simultaneously, triggered by the ferromagnetic ordering, the *I-M* transition would be more severe and accomplished within a narrow temperature range, leading to the steep drop of resistivity. Also, in such a form of phase separation, it would be much easier for an applied magnetic field to trigger a collective percolation of isolated metallic clusters. In addition, because the extra magnetic coupling induced by Gd^{3+} can be tuned

by external field, the microscopic magnetic structure, and consequently the size of metallic ferromagnetic clusters, are more sensitive to applied magnetic field. Due to above points, the CMR is greatly enhanced in $(La_{0.7-x}Gd_x)Sr_{0.3}MnO_3$.

V. CONCLUSION

The influences of Gd substitution in $La_{0.7}Sr_{0.3}MnO_3$ have been studied. The substitution of Gd on La sites not only results in the decrease of Curie temperature T_c and the magnetization, but also induces cluster-glass and ferrimagnetic behaviors. The insulating-metallic transition shifts to lower temperature with increasing Gd content and the *I-M* transiton temperature disagrees with Curie temperature T_c when $x > 0.2$. Both the high-field and low-field magnetoresistance are significantly enhanced by Gd substitution. Infrared pho-

non spectra reveal the change of Mn-O-Mn bond angle, but not bond length, due to Gd substitution. These results suggest that both the average *A*-site ionic radius (tolorence factor) and the extra magnetic coupling between Gd^{3+} and Mn^{3+}/Mn^{4+} sublattice are important factors in determining the magnetic and electronic states. The enhancement of CMR and *I-M* transition are interpreted in terms of the phase separation.

[1] R. von Helmolt, J. Wecker, B. Holzapfel, L. Schultz, and K. Samwer, Phys. Rev. Lett. **71**, 2331 (1993).

[2] S. Jin, T.H. Tiefel, M. McCormack, R.A. Fastnacht, R. Ramesh, and L.H. Chen, Science **264**, 413 (1994).

[3] P. Schiffer, A.P. Ramirez, W. Bao, and S.-W. Cheong, Phys. Rev. Lett. **75**, 3336 (1995).

[4] Y. Yamada, O. Hino, S. Nohdo, R. Kanao, T. Inami, and S. Katano, Phys. Rev. Lett. **77**, 904 (1996).

[5] H. Kuwahara, Y. Tomioka, A. Asamitsu, Y. Moritomo, and Y. Tokura, Science **270**, 961 (1995).

[6] P.G. Radaelli, D.E. Cox, M. Marezio, and S-W. Cheong, Phys. Rev. B **55**, 3015 (1997).

[7] H. Meskine, H. Konig, and S. Satpathy, Phys. Rev. B **64**, 094433 (2001).

[8] Adriana Moreo, Seiji Yunoki, and Elbio Dagotto, Science **283**, 2034 (1999).

[9] M. Fäth, S. Freisem, A.A. Menovsky, Y. Tomioka, J. Aarts, and J.A. Mydosh, Science **285**, 1540 (1999).

[10] M. Jaime, P. Lin, S. Chun, M. Salamon, P. Dorsey, and M. Rubinstein, Phys. Rev. B **60**, 1028 (1999).

[11] C. Zener, Phys. Rev. **82**, 403 (1951); P.W. Anderson and H. Hasegawa, *ibid.* **100**, 675 (1955).

[12] A.J. Millis, P.B. Littlewood, and B.I. Shraiman, Phys. Rev. Lett. **74**, 5144 (1995).

[13] H.Y. Hwang, S.-W. Cheong, P.G. Radaelli, M. Marezio, and B. Batlogg, Phys. Rev. Lett. **75**, 914 (1995).

[14] T. Terai, T. Kakeshita, T. Fukuda, T. Saburi, N. Takamoto, K. Kindo, and M. Honda, Phys. Rev. B **58**, 14 908 (1998).

[15] Hirotoshi Terashita and J.J. Neumeier, Phys. Rev. B **63**, 174436 (2001).

[16] J.P. Zhou, J.T. McDevitt, J.S. Zhou, H.Q. Yin, J.B. Goodenough, Y. Gim, and Q.X. Jia, Appl. Phys. Lett. **75**, 1146 (1999).

[17] J.A. Mydosh, *Spin Glass: An Experimental Introduction* (Taylor and Francis, London, 1993).

[18] Z.B. Guo, H. Huang, W.P. Ding, and Y.W. Du, Phys. Rev. B **56**, 10 789 (1997).

[19] G.J. Snyder, C.H. Booth, F. Bridges, R. Hiskes, S. DiCarolis, M.R. Beasley, and T.H. Geballe, Phys. Rev. B **55**, 6453 (1997).

[20] D. Emin and T. Holstein, Phys. Rev. B **13**, 647 (1976).

[21] N.F. Mott and E.A. Davies, *Electronic Processes in Noncrystalline Materials* (Oxford University Press, Oxford, 1971).

[22] A. Goyal, M. Rajeswari, R. Shreekala, S.E. Lofland, S.M. Bhagat, T. Boettcher, C. Kwon, R. Ramesh, and T. Venkatesan, Appl. Phys. Lett. **71**, 2535 (1997).

[23] R. Shreekala, M. Rajeswari, S.P. Pai, S.E. Lofland, V. Smolyaninova, K. Ghosh, S.B. Ogale, S.M. Bhagat, M.J. Downes, R.L. Greene, R. Ramesh, and T. Venkatesan, Appl. Phys. Lett. **74**, 2857 (1999).

[24] Ravi Bathe, K.P. Adhi, S.I. Patil, G. Marest, B. Hannoyer, and S.B. Ogale, Appl. Phys. Lett. **76**, 2104 (2000).

[25] K.H. Kim, J.Y. Gu, H.S. Choi, G.W. Park, and T.W. Noh, Phys. Rev. Lett. **77**, 1877 (1996).

[26] M. Uehara, S. Mori, C.H. Chen, and S.-W. Cheong, Nature (London) **399**, 560 (1999).

[27] E. Dagotto, T. Hotta, and A. Moreo, Phys. Rep. **344**, 1 (2001).

[28] A. Yakubovskii, K. Kumagai, Y. Furukawa, N. Babushkina, A. Taldenkov, A. Kaul, and O. Gorbenko, Phys. Rev. B **62**, 5337 (2000).

[29] I.G. Deac, J.F. Mitchell, and P. Schiffer, Phys. Rev. B **63**, 172408 (2001).

[30] M.B. Salamon, P. Lin, and S.H. Chun, Phys. Rev. Lett. **88**, 197203 (2002).

[31] A.J. Millis, B.I. Shraiman, and R. Mueller, Phys. Rev. Lett. **77**, 175 (1996).